Journal of Science and Transport Technology
Journal homepage: https://jstt.vn/index.php/en

Cross-Branch CNN-MLP Integration for Improving Landslide Spatial Probability on Mt. Umyeon, Korea

Ba-Quang-Vinh Nguyen[1,2,*], Tan-Hung Nguyen[3], Van-Hiep Le[4]
[1]School of Civil Engineering and Management, International University, VNU-HCM, Ho Chi Minh City, Vietnam
[2]Vietnam National University, Ho Chi Minh City, Vietnam
[3]Faculty of Architectural, Civil and Environmental Engineering, Nam Can Tho University, 168 Nguyen Van Cu Street, An Binh Ward, Can Tho City, Vietnam
[4]Geotechnical and Artificial Intelligence research group, University of Transport Technology, Ha Noi 100000, Vietnam

Article info
Type of article:
Original research paper

DOI:
https://doi.org/10.58845/jstt.utt.2026.en.6.1.183-198

***Corresponding author:**
Email address:
nbqvinh@hcmiu.edu.vn

Received: 12/09/2025
Received in Revised Form: 21/11/2025
Accepted: 25/11/2025

Abstract: Accurate maps of landslide spatial probability (LSP) are crucial for planning and risk reduction in steep, urbanized areas. A hybrid Convolutional Neural Network (CNN) - Multilayer Perceptron (MLP) model is introduced for mapping LSP in Mt. Umyeon, Korea. The design combines two complementary views of each location: a convolutional branch learns spatial context from multi-channel image patches. At the same time, a multilayer perceptron captures local numeric and categorical attributes at the central point. Feature-level fusion concatenates the embeddings from both branches and feeds a lightweight classifier to produce probabilities. Performance was assessed under consistent data splits and training protocols. Training AUCs reached 0.887 (MLP), 0.894 (CNN), and 0.903 (CNN-MLP). More importantly, validation AUCs were 0.808 (MLP), 0.821 (CNN), and 0.854 (CNN-MLP), indicating stronger generalization for the fused representation. These gains reflect the complementary nature of neighborhood structure learned by the CNN and pointwise information stabilized by the MLP. The results show that a compact, feature-level fusion of CNN and MLP can materially improve spatial probability mapping of landslides. The approach provides a practical route to more reliable probability surfaces for decision support in mountainous urban regions.

Keywords: Convolutional neural network, Feature level fusion, Landslide spatial probability, Multilayer perceptron, Mt. Umyeon.

1. Introduction

Landslides are a major hazard in mountainous terrain, causing substantial losses and fatalities, especially in areas with high population density. Estimating the spatial probability of landslide occurrence is therefore essential for mitigation, land-use planning, and emergency response. Contemporary approaches typically integrate mapped landslide inventories with conditioning factors (CFs) that represent the principal physical controls: topographic, hydrological, soil, geological, and environmental variables, to quantify where landslides are more likely to occur. Over the past decades, such

inventory-based, data-driven models have received sustained attention and now underpin many operational assessments of landslide occurrence [1], [2], [3], [4], [5].

Spatial probability analysis is a practical and rigorous way to identify zones with a high likelihood of landslides [6], [7]. In recent decades, advances in data and computing have enabled many approaches for estimating landslide spatial probability (LSP), with machine learning (ML) increasingly used in geohazard and civil engineering applications [5], [3], [8], [9]. ML methods commonly applied to probabilistic mapping include logistic regression (LR) [1], [10], [11] naïve Bayes (NB) [5], [11], [12], [13] decision trees (DT) [13], [12], [10] and artificial neural networks (ANN) [10], [11], [5]. Recent studies further demonstrate that these techniques can achieve strong performance in mapping landslide spatial probability [5], [11], [12], [13]. However, model choice remains critical for high accuracy. Performance depends on data quality, representation of conditioning factors, class imbalance, spatial autocorrelation, and the validation design. Careful selection, calibration, and evaluation of ML models are therefore essential to produce reliable probability maps for decision support [1].

Single model machine learning methods have been widely used to estimate landslide spatial probability. However, yet each has practical limits: tabular models often miss neighborhood context, while image-based models can weaken categorical semantics from conditioning factors. These gaps motivate hybrid ML designs that combine complementary representations for predicting LSP [1], [14], [15]. Across studies, such hybrids tend to improve discrimination and calibration by capturing both local attributes and neighborhood structure while mitigating model-specific biases.

Recent work has intensively examined landslide spatial probability at Mt. Umyeon, Korea [5], [4], [16]. However, most studies rely on single-model ML approaches, which can underuse neighborhood context or categorical semantics in conditioning factors. Given the site's complex terrain and mixed data types, further research on hybrid ML frameworks that fuse complementary representations remains necessary to improve LSP accuracy and robustness in this area.

Motivated by limitations of single-model ML in landslide spatial probability mapping at Mt. Umyeon, this study adopts a hybrid Convolutional Neural Network (CNN) - Multilayer Perceptron (MLP) design. The core idea is to combine two complementary sources of information: a CNN learns spatial context from the neighborhood around each location, while an MLP preserves site-specific attributes at the same point. By fusing these representations at the feature level, the model aims to improve discrimination and deliver more reliable probability estimates than either branch alone, while remaining compatible with standard landslide inventory and CFs workflows. Performance is evaluated using receiver operating characteristic (ROC) analysis, reporting the area under the curve (AUC) for both training and validation sets.

2. Methods

In this study, a hybrid learning framework is introduced to improve the accuracy of landslide spatial probability mapping. The workflow (Fig. 1) includes:

i. Compilation of a verified landslide inventory and partitioning into training and test sets;

ii. Identification of relevant conditioning factors;

iii. Examination of inter-factor relationships using multicollinearity diagnostics;

iv. Training of three predictors: an MLP that uses point-level tabular attributes, a CNN that uses local multi-channel patches to capture neighborhood context, and a feature-level CNN-MLP fusion that concatenates both representations before classification to estimate location-wise LSP;

v. Evaluation of predictive performance using receiver operating characteristic analysis, reported by the area under the curve.

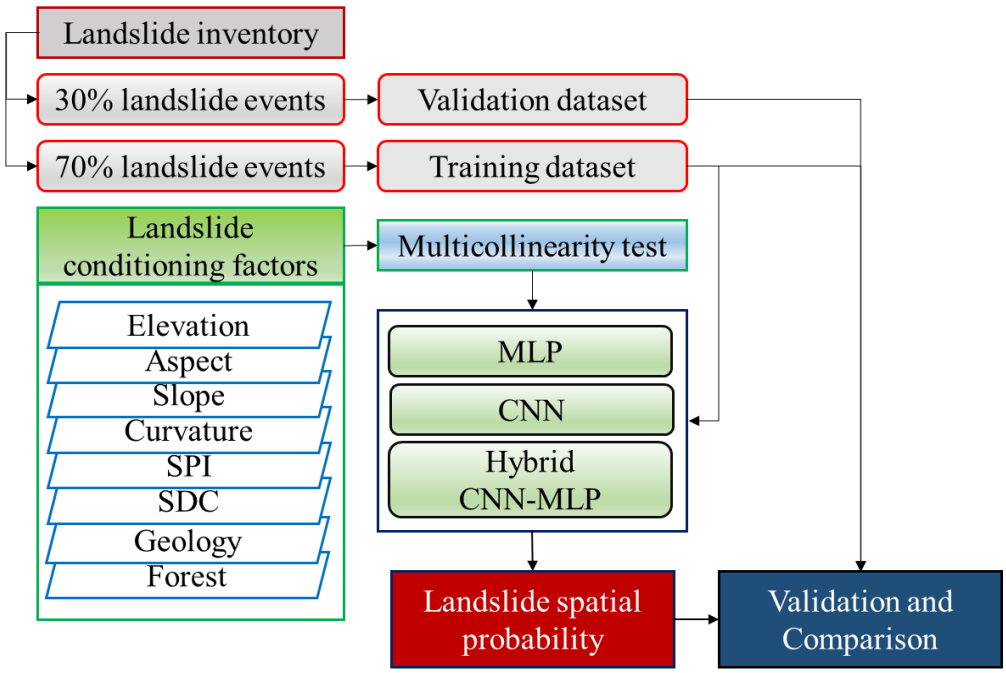

Fig. 1. Schematic workflow for landslide spatial probability mapping

2.1. Multicolinearity tests

Correlations among CFs can bias estimates and reduce predictive accuracy [5], [17]. To address this risk, multicollinearity was examined for all conditioning factors using tolerance (TOL) and the variance inflation factor (VIF) [5], [18]. Following widely used guidelines, VIF < 10 (equivalently TOL > 0.1) was interpreted as acceptable collinearity for subsequent landslide spatial-probability modeling [3]. These diagnostics provide a clear, transparent screen that helps prevent unstable coefficients and misleading model interpretations.

2.2. Multilayer perceptron

Multilayer perceptron is feed forward neural networks that learn nonlinear mappings by composing affine layers with pointwise activations [19], [20]. A typical MLP for landslide spatial probability prediction includes: (i) an input layer whose size equals the number of conditioning factors at a location; (ii) one or more hidden layers that transform inputs into higher level features; and (iii) an output layer that produces a probability for landslide or non-landslide. Standardization of continuous factors and one hot encoding of categorical variables improve numerical stability; optional batch normalization can further stabilize training. Hyperparameter selection is performed using spatial cross validation to minimize leakage from nearby samples [21]. Key choices include network depth/width, activation function, weight initialization, optimizer, learning rate, batch size, and regularization [22], [23]. Training is typically monitored with early stopping to prevent overfitting.

2.3. Convolutional neural network

Convolutional neural networks (CNNs) are a central family of deep learning models that achieve state-of-the-art results in visual pattern recognition [24], [25]. Conceptually, a CNN extends the multilayer perceptron by introducing convolutional blocks that learn spatial filters, typically arranged with nonlinear activations and, when appropriate, pooling operations to enlarge the receptive field while controlling resolution. A classification head, usually composed of one or more fully connected layers, then maps the learned representation to the target output. This canonical organization consists of an input stage, followed by convolution, normalization, and activation, with pooling where appropriate, then a fully connected head, and finally the output, and it is widely adopted across imaging applications [26]. For landslide spatial probability analysis, CNN processes small multi-band neighborhoods of conditioning factors around

each location to learn terrain patterns that are strongly associated with landslide occurrence. The hierarchy of convolutional blocks extracts increasingly abstract spatial features, which a lightweight head converts into a probability for the target site. This design captures neighborhood structure while remaining compact and data efficient. Instead of fixing hyperparameters in advance, model depth and width, neighborhood window size, and regularization are selected through validation with spatial cross validation. Performance is tracked using AUC, and early stopping is applied when the validation metric no longer improves, which helps control overfitting [21].

2.4. Hybrid CNN-MLP

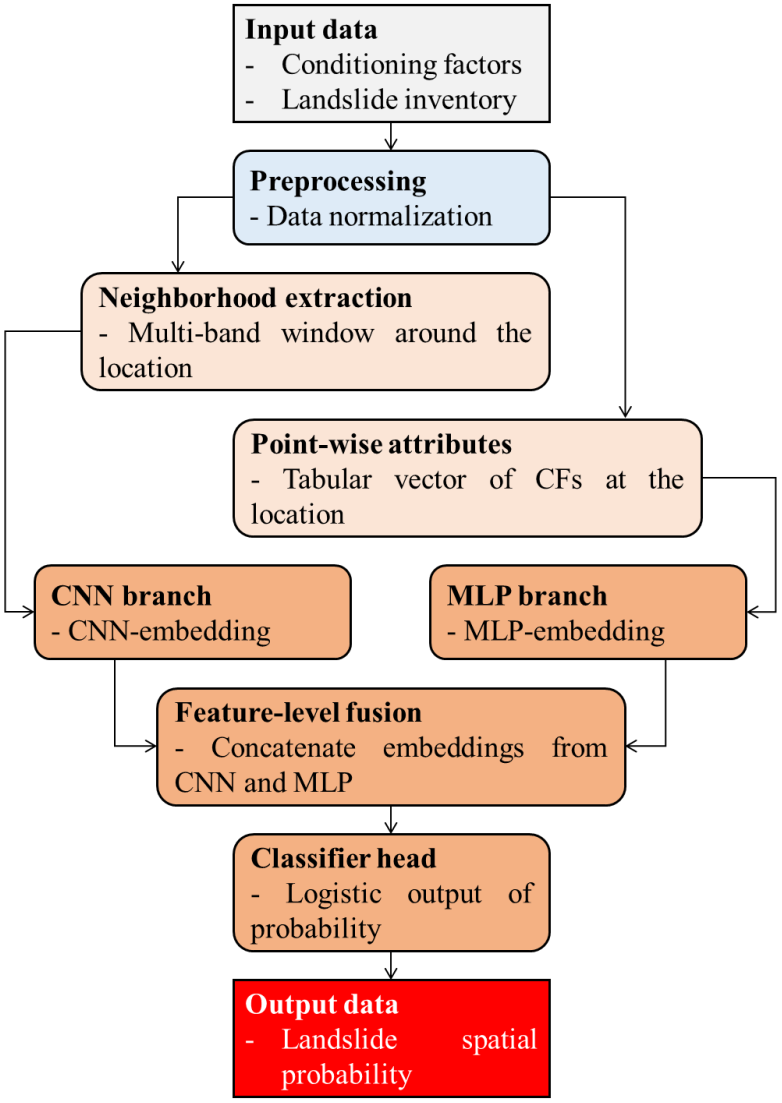

Fig. 2. CNN-MLP fusion architecture for landslide spatial probability estimation

A hybrid CNN-MLP architecture is adopted to estimate landslide spatial probability by combining neighborhood context with site-specific attributes at each location. A convolutional branch processes a small multiband neighborhood of conditioning factors to learn terrain patterns associated with landslide occurrence, while a multilayer perceptron simultaneously transforms the co-located tabular factors, preserving numeric magnitudes and categorical semantics. The resulting embeddings are concatenated at the feature level and passed to a compact classification head that outputs the probability at the target site. This fusion leverages complementary information, including spatial structure from the CNN and point attributes from the MLP, yielding a compact and data-efficient

model that typically improves discrimination and reliability relative to single-branch baselines. Training uses binary cross-entropy with class weighting when needed, and performance is monitored by AUC with early stopping to curb overfitting; hyperparameters are selected via Bayesian optimization within a spatial cross-validation framework. This combined method guarantees the model's computational efficiency and strong predictive generalization across geographically separate regions [21]. Key choices include the CNN depth and channel width, the MLP hidden layers and units, the fusion dimension, the neighborhood window size, the optimizer and learning-rate, and regularization through weight decay and dropout. The optimized hyperparameter values are presented in Table 1. Details of this hybrid technique are shown in Fig. 2.

Table 1. The used hyperparameters

Hyperparameter	MLP	CNN	Fusion head
Number of hidden layers	1	N/A	1
Convolutional layers	N/A	3	N/A
Neurons/Filters	128	32, 64, 128	128
Kernel size	N/A	3x3	N/A
Activation function	ReLU	ReLU	ReLU
Pooling layer	N/A	Max Pooling (2x2)	N/A
Dropout rate	0.2	0.2	0.3
Optimizer	Adam	Adam	Adam
Learning rate	1e-3	1e-3	1e-3
Weight decay	1e-4	1e-4	1e-4
Batch size	128	128	128
Epochs	200	200	200
Fusion dimension	N/A	N/A	192

2.5. Receiver operating characteristic analysis

Rigorous validation is essential for landslide spatial probability assessment. This study evaluates model discrimination using receiver operating characteristic analysis, summarised by the area under the curve, a threshold-free metric widely adopted in recent work [4], [5], [16], [27]. AUC ranges from 0 to 1, with larger values indicating stronger separation between landslide and non-landslide locations. In addition, we report the success-rate curve (SRC) and the prediction-rate curve (PRC). The SRC measures goodness-of-fit by comparing the spatial probability map with the training inventory used for model fitting, whereas the PRC quantifies generalization by overlaying the map with a held-out landslide inventory. Together, AUC, SRC, and PRC provide complementary evidence on in-sample fit and out-of-sample predictive performance.

3. Study area and data preparations

3.1. Study area

Mt. Umyeon occupies approximately 6.8 km² on the southern margin of Seoul, Korea (37.45-37.48° N; 126.90-127.04° E) (Fig. 3). The study area is primarily covered by dense, diverse forest, including coniferous and deciduous species along with understory vegetation. Topographically, the region is rugged, featuring steep hills, gullies, and valleys, with elevations ranging from 20 m to 312 m above mean sea level (amsl). The underlying bedrock is intensely weathered and heavily fractured, and is typically blanketed by a layer of colluvium. A high groundwater level is inferred within the basin, evidenced by six mineral springs concentrated on the slope at an altitude between 220 m and 250 m. Mean annual precipitation ranges from 1100 to 1500 mm, with about 70% of rainfall concentrated in the June-September

monsoon season. On 27 July 2011, a severe landslide episode affected Mt. Umyeon. The failure mechanism mainly involved shallow landslides (estimated average depth of 1.0 to 1.5 meters within the soil mantle or colluvium) that rapidly transformed into destructive debris flows. The total estimated volume of material lost and transported by the debris flow was about 38,000 cubic meters [28]. This large movement of material heavily affected densely populated areas downslope, causing multiple fatalities and extensive damage to infrastructure. Direct economic losses were roughly estimated at $15 million.

3.2. Landslide inventory

Following the 2011 landslide, detailed field and remote sensing surveys were carried out to map the resulting slope failures. Specifically, 163 landslide source areas (Fig. 3) were identified using 1:5,000 topographic maps, recent satellite images, and targeted field inspections. These features were then compiled into a comprehensive, georeferenced landslide inventory, which later served as the key response variable for the spatial-probability modeling. For out-of-sample evaluation, the inventory was randomly partitioned at a 70:30 ratio into training and validation subsets.

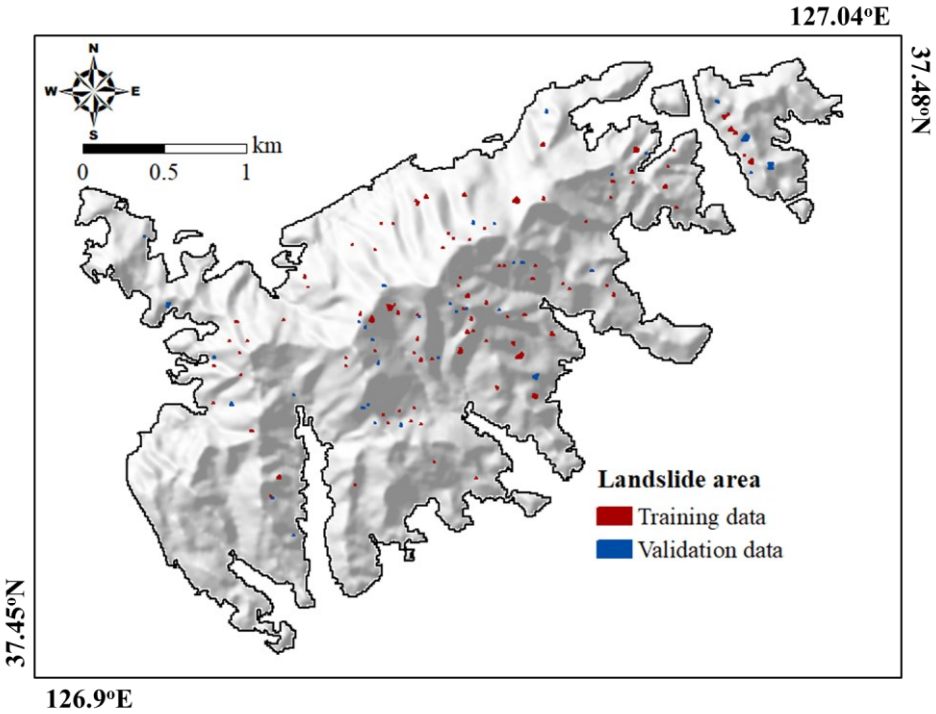

Fig. 3. Landslide inventory in Mt. Umyeon, Korea

The number of non-landslide locations used in the training set was systematically varied, starting from a 1:1 ratio (equal to the number of landslide features) and increasing to higher proportions, up to the maximum available within the study area. These negative samples were selected randomly. The model was trained and evaluated separately for each ratio, and the configuration that produced the highest predictive accuracy was ultimately chosen as the best training dataset for generating the final LSP map.

3.3. Conditioning factors

Eight conditioning factors were assembled to model landslide spatial probability at Mt. Umyeon. Terrain-derived variables were computed from a 10 m × 10 m digital elevation model provided by the National Geographic Information Institute, and categorical layers were taken from prior studies [1], [5]. The CFs and their mapped ranges or classes (Figs. 4a–h) are:

Elevation (Fig. 4a) is a common conditioning factor in landslide studies, reflecting broader controls on climate, weathering depth, and human activity. Prior work has reported increasing

landslide likelihood at greater heights [29]. At Mt. Umyeon, elevation ranges from 20.5 to 311.5 m a.m.s.l.

Aspect (Fig. 4b) describes the azimuth of slope orientation and influences insolation, evapotranspiration, prevailing winds, and rain exposure. In this study, aspect is treated as a continuous circular variable from 0–360°.

Slope (Fig. 4c) is a primary control on stability, as steeper gradients increase driving stresses relative to resisting forces. Within the study area, slopes vary from 0.078° to 46.4°, covering gentle foothills to steep scarps.

Curvature (Fig. 4d) is the second derivative of the land surface and distinguishes concave zones that concentrate flow and pore pressure from convex zones that disperse it. Values in the study area range from -13.4 (strongly concave) to 12.8 (strongly convex). This factor is particularly informative in steep terrain where micro-topography modulates stability.

Stream Power Index (SPI) (Fig. 4e) approximates the energy available for erosion by combining upslope contributing area with local slope, thereby highlighting hollows and channelized pathways where shear stresses and sediment transport are elevated. In Mt. Umyeon, SPI spans 0-514.8, with higher values marking potential flow corridors and initiation sites for mass movement.

Soil Drainage Characteristics (SDC) (Fig. 4f) represents how frequently and for how long soils approach saturation, which affects effective stress and shear strength. Following [5], the area is classified into four classes: very poor, poor, moderate, and well-drained.

Geology (Fig. 4g) governs contrasts in strength, fabric, jointing, and weathering that shape failure mechanisms. Based on [5], the study area includes four mapped units: Jdgr, PCEggn, PCEbngn, and PCElgn.

Forest cover (Fig. 4h) influences root reinforcement, canopy interception, and evapotranspiration, thereby modulating near-surface hydrology and strength. The forest map [5] distinguishes four classes: scattered, conifer, broadleaf, and mixed.

At Mt. Umyeon, there is a clear spatial difference: residential areas and major road networks are mainly located at the mountain's base and lower slopes, while recorded landslide events are scattered across higher slopes [28]. Importantly, these failures showed no clear spatial link with road cuts or transportation infrastructure. As a result, the road network was excluded from the LSP model, allowing the analysis to focus solely on natural factors that directly influence the shallow landslide failure mechanism.

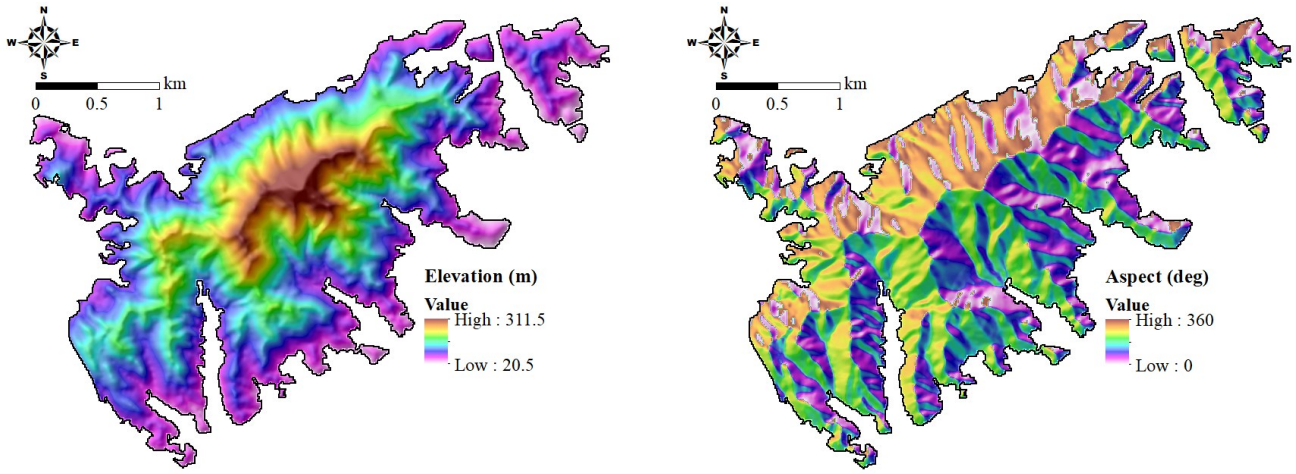

(a) (b)

Fig. 4. Conditioning factors in Mt. Umyeon, Seoul, Korea used as input data: (a) elevation, (b) aspect, (c) slope, (d) curvature, (e) SPI, (f) SDC, (g) geology, (h) forest

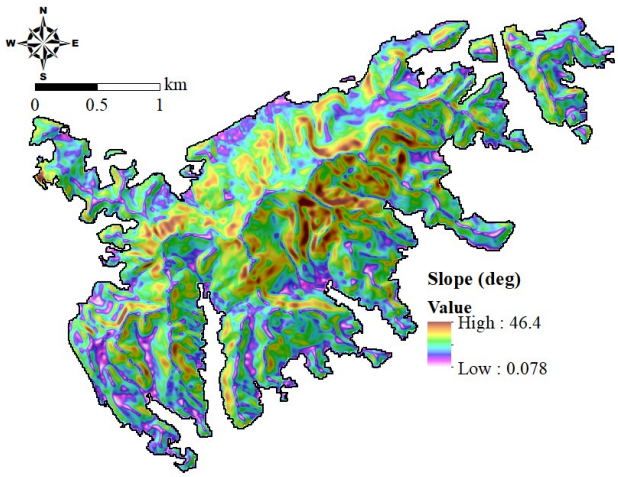

(c)

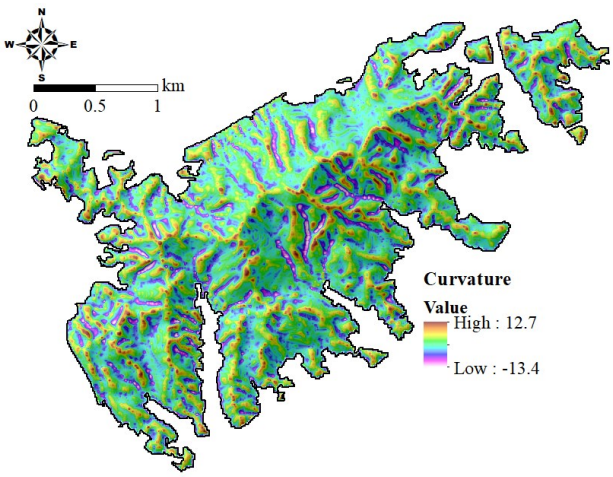

(d)

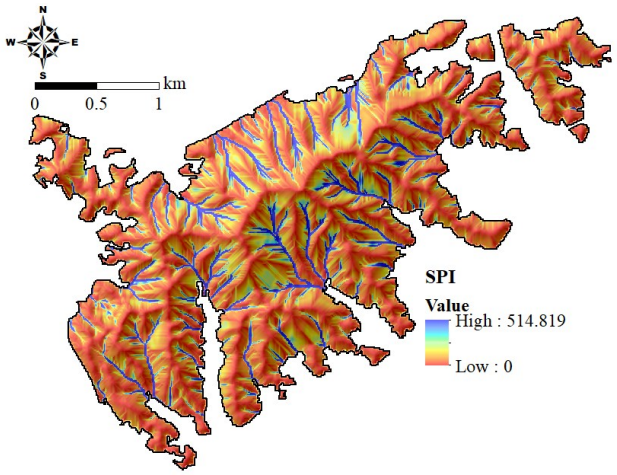

(e)

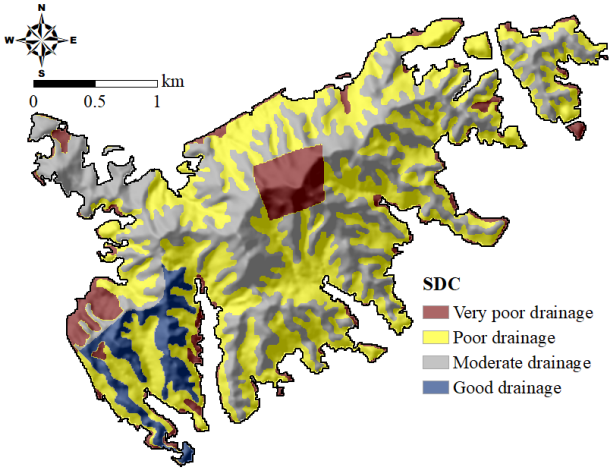

(f)

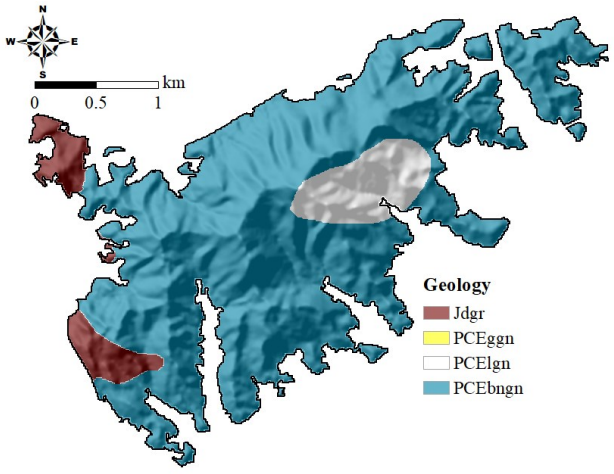

(g)

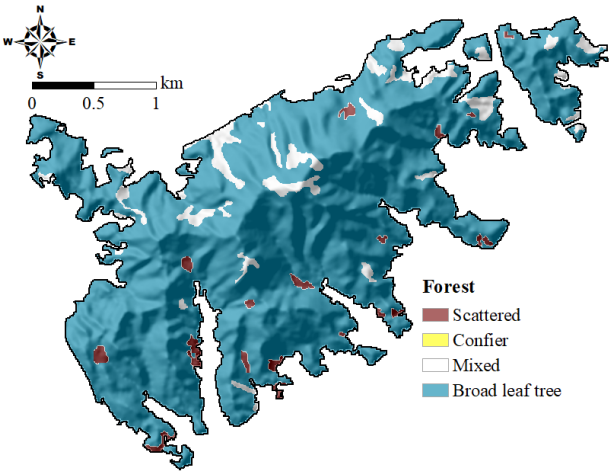

(h)

Fig. 4. (continued)

3.4. Normalization of conditioning factors

All conditioning factors were normalized to improve numerical stability, ensure comparable scaling, and prevent information leakage. The topographic metrics, including elevation, slope, aspect, and curvature, were treated as a unified set of continuous variables. In which, elevation, slope, and curvature were standardized using z-scores (subtract the training mean and divide by the training standard deviation to obtain variables with

mean around zero and unit variance), then applied unchanged to validation. Because aspect is circular ($0^{o} \equiv 360^{o}$), it was first encoded as sine and cosine to avoid artificial discontinuities; each channel was then standardized with training-set statistics. SPI often exhibit right-skewed distributions; this was transformed using log1p ($y=\log(1+x)$) to compress heavy tails while remaining defined at zero, and subsequently standardized with z-scores. Categorical factors (SDC, geology, and forest) were represented via one-hot encoding, which maps each class to a separate binary indicator column without imposing an artificial order; these indicators were left unscaled. All preprocessing parameters (means, standard deviations, and categorical vocabularies) were saved and reused for both CNN and MLP branches to maintain consistent representations and ensure reproducibility.

4. Results

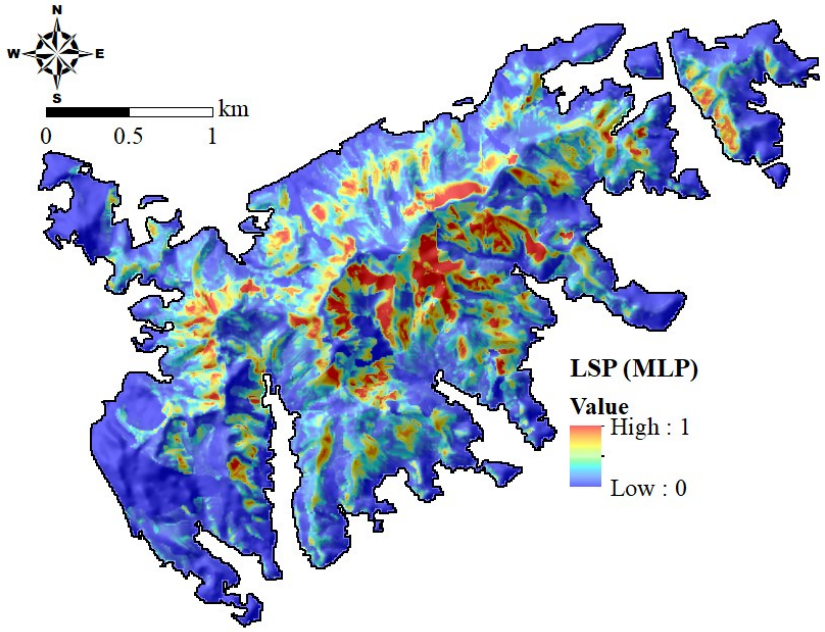

(a)

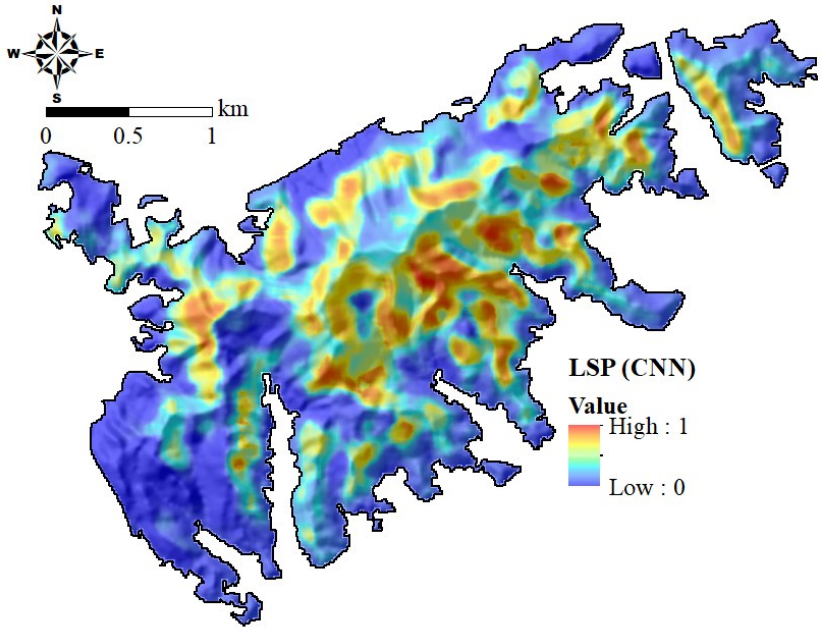

(b)

Fig. 5. Landslide spatial probability map at Mt. Umyeon, Korea: (a) MLP model, (b) CNN model, (c) Hybrid CNN-MLP model

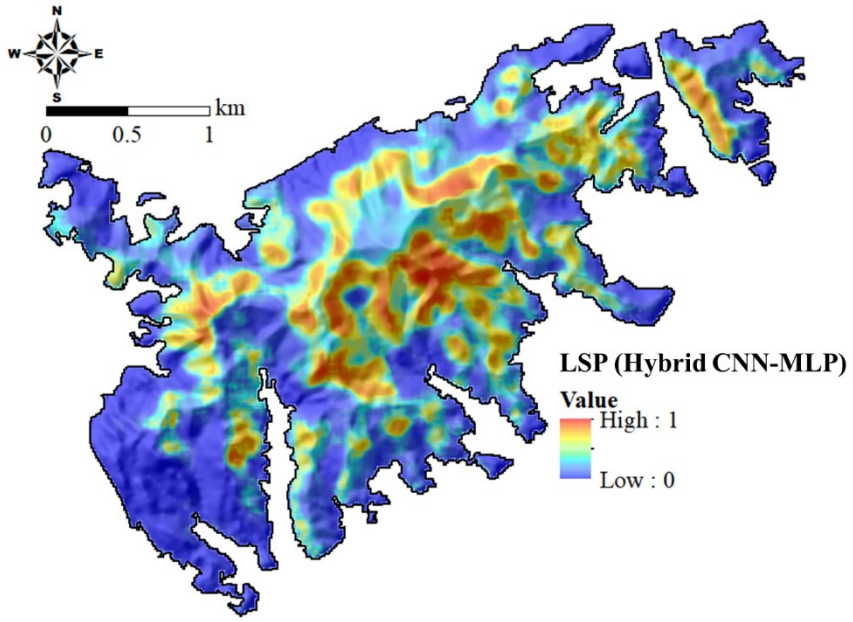

(c)

Fig. 5. (continued)

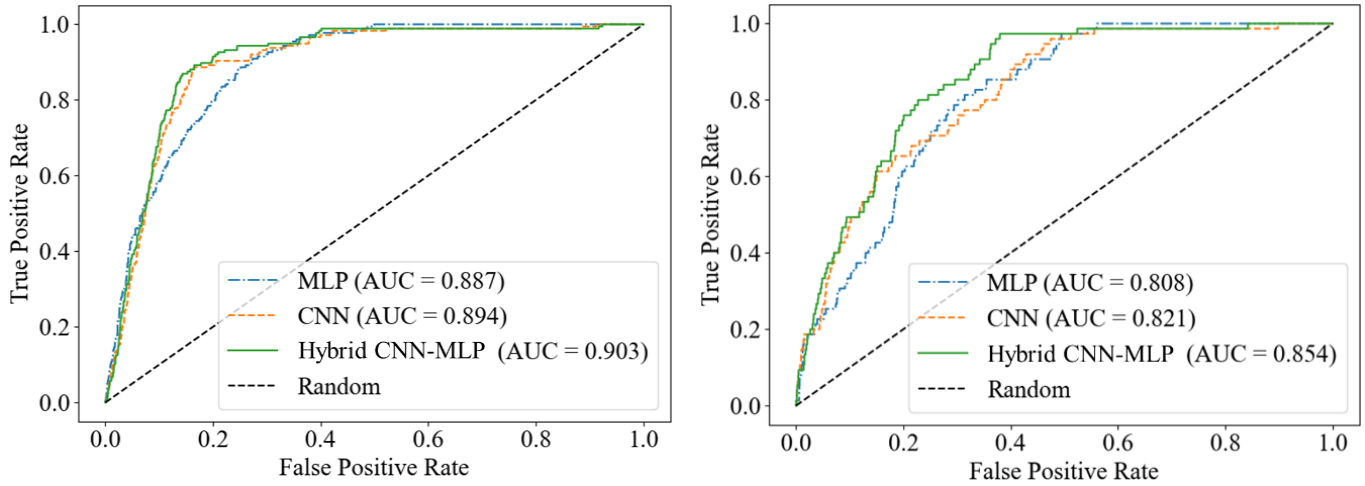

(a) (b)

Fig. 6. ROC curves: (a) Success-rate curve (SRC), (b) Predicted-rate curve (PRC)

Multicollinearity diagnostics indicate no problematic interdependence among the landslide CFs at this site. VIF ranges from 1.016 to 1.555 and TOL from 0.643 to 0.984. All values satisfy common acceptability criteria (VIF < 10 or TOL > 0.1), indicating no evidence of severe collinearity and supporting the inclusion of all CFs in subsequent modeling.

Figs. 5a-5c present three spatial probability maps derived from the MLP, CNN, and the hybrid CNN-MLP models, respectively. Probabilities span the full range from low (0) to high (1), delineating zones of elevated landslide likelihood across the study area. The corresponding SRC–AUC and PRC–AUC analyses (Fig. 6) summarize the model's discrimination performance on both the training (Fig. 6a) and validation (Fig. 6b) datasets. The SRC–AUC values for the training phase are 0.887 for the MLP, 0.894 for the CNN, and 0.903 for the hybrid CNN–MLP model, while the PRC–AUC values for the validation phase are 0.808, 0.821, and 0.854, respectively. These results indicate that all three models successfully discriminate landslide versus non-landslide locations for LSP mapping, while the hybrid CNN-MLP achieves the highest AUCs and the strongest generalization, highlighting the benefit of combining neighborhood context with site-specific

attributes.

Permutation importance (PI) was used to quantify how much each conditioning factor contributes to the landslide spatial probability predictions. For each factor, values were randomly permuted on the validation set while keeping the fitted model fixed, and the decrease in AUC relative to the baseline was recorded. Larger AUC drops indicate greater dependence of the LSP model on that factor [30], [31]. Results (Fig. 7) reveal a clear hierarchy: elevation exerts the strongest influence (PI is about 0.20); slope and SDC follow with comparable effects (PI is about 0.15-0.16); geology ranks next (PI is about 0.11-0.12); aspect and forest cover make moderate contributions (PI is about 0.07-0.08); curvature and SPI are smaller but non-negligible (PI is about 0.03-0.04). Narrow error bars indicate a stable ordering across repetitions. This pattern accords with process understanding and prior syntheses of landslide susceptibility: relief and gradient are primary controls, subsurface drainage strongly modulates pore pressure and triggering, and lithology governs contrasts in shear strength and jointing; directional exposure, vegetation, and fine scale surface shape tend to act as secondary modifiers of susceptibility [32], [33]. Hydrologic interpretations are consistent with physically based arguments linking rainfall infiltration, contributing area, and slope to failure potential [34], [35], while the roles of aspect and forest align with documented effects on moisture, interception, evapotranspiration, and root reinforcement [36]

5. Discussions

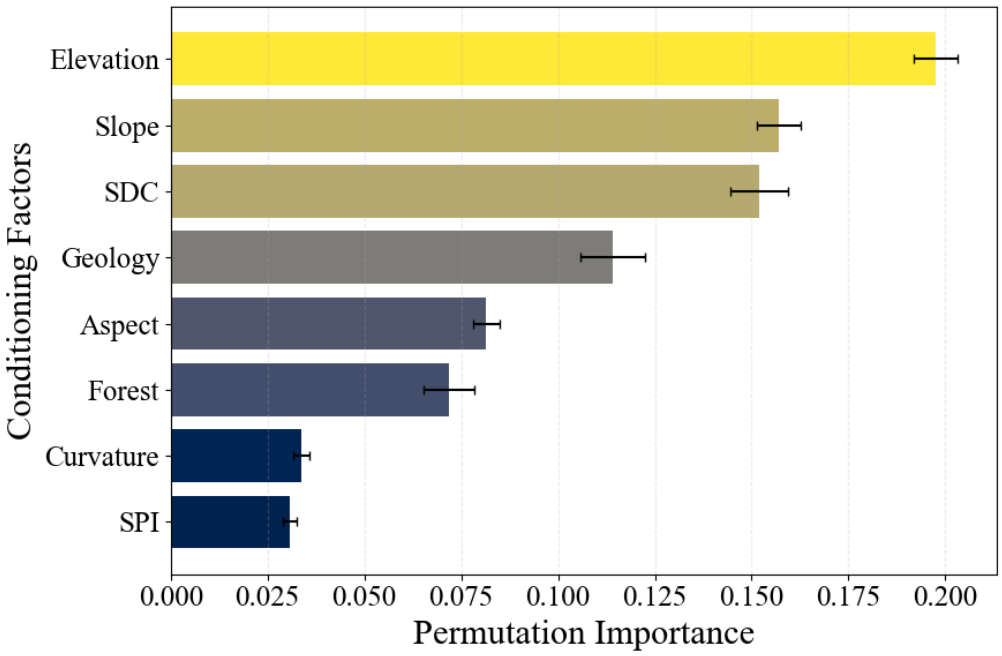

Fig. 7. Feature importance

The three LSP maps display a broadly consistent pattern: higher probabilities concentrate over the dissected interior hills, whereas the lower-relief margins remain predominantly low. The MLP map exhibits the finest spatial texture, with many small, isolated hotspots that reflect strong reliance on site-specific attributes but also introduce a speckled appearance. The CNN map is smoother and more spatially coherent, organizing high-probability areas into elongated belts that align with terrain structure, though some local peaks are subdued. The CNN-MLP fusion strikes a balance between these behaviors. It preserves the CNN's coherent belts while retaining sharper local maxima from the tabular signal, producing clearer boundaries and more plausible extents of high probability. Areas of agreement across all three maps cluster in the central high-relief sector; divergences arise mainly in transition zones, where the MLP expands fragmented hotspots and the

CNN constrains responses to linear corridors. This spatial behavior is consistent with the AUC results: all models deliver credible LSP patterns, and the hybrid provides the most discriminative and visually coherent surface.

The SRC-AUC and PRC-AUC values provide essential insights into the spatial predictive ability of the models. A higher SRC-AUC during training indicates that the model is more effective at ranking observed landslide locations above non-landslide areas in the calibration dataset, while a higher PRC-AUC in the validation or prediction phase reflects better identification and prioritization of zones with high predicted susceptibility in unseen areas. In this study, the hybrid CNN-MLP model achieved the highest scores for both metrics, demonstrating its superior capacity to capture local spatial patterns from raster patches and attribute-based variations from tabular features.

The ordering of AUC across models: highest for the hybrid CNN-MLP, next for CNN, and lowest for MLP, reflects how each approach captures information for landslide spatial probability. The multilayer perceptron uses site-specific tabular factors and therefore cannot learn neighborhood morphology such as ridges, hollows, channels, and slope breaks. The convolutional neural network adds spatial context by learning patterns in the surrounding terrain, which usually improves discrimination over tabular models but may underuse categorical meaning and precise point values. The hybrid model combines the two representations at the feature level so the classifier can use neighborhood structure together with site attributes and can learn their interactions. This early-fusion design reduces blind spots present in single branches and tends to improve generalization and probability calibration. These findings are consistent with evidence on stacking and early fusion, multimodal learning, and spatial representation learning in imaging and remote sensing [37], [38], [39].

In landslide spatial probability prediction, the three architectures exhibit a clear trade-off between predictive performance, computational time, and model complexity. The multilayer perceptron is the simplest and fastest configuration: using only site-specific conditioning factors, it achieved AUC values of 0.887 for training data and 0.808 for validation data with a wall-clock time of approximately 60s. The convolutional neural network adds neighborhood context learned from local terrain patterns and, accordingly, improved discrimination to 0.894 for training set and 0.821 for validation set, but at substantially higher cost due to convolution and data handling, requiring about 4,260s. The hybrid CNN-MLP fuses spatial context with tabular attributes at the feature level and yielded the strongest results: 0.903 for training data and 0.854 for validation data, together with the most spatially coherent maps; however, it also incurred the greatest computational burden, with a runtime near 6,060s. In sum, MLP favors speed and simplicity, CNN offers a balanced compromise when spatial structure matters, and CNN-MLP is preferred when maximizing accuracy and map quality justifies additional time and complexity.

6. Conclusions

This study mapped landslide spatial probability at Mt. Umyeon using three approaches, including a MLP model, a CNN model, and a feature-level CNN-MLP fusion. The maps were derived from a landslide inventory and eight conditioning factors. These factors are elevation, aspect, slope, curvature, stream power index, soil drainage characteristics, geology, and forest cover. All factors were processed in a consistent way then were assessed multicollinearity using variance inflation factor and tolerance.

The area under the receiver operating characteristic curve on the training data was 0.887 for the multilayer perceptron, 0.894 for the convolutional neural network, and 0.903 for the hybrid. On the validation data the values were 0.808 for the multilayer perceptron, 0.821 for the convolutional neural network, and 0.854 for the

hybrid. These results show that all three models successfully constructed credible landslide spatial probability maps, with the hybrid providing the strongest overall performance and the most consistent generalization.

The landslide spatial probability maps differ systematically across models. The multilayer perceptron yields fine-grained but fragmented patterns with many small hotspots, reflecting strong reliance on site attributes and sensitivity to local noise. The convolutional neural network produces smoother, more coherent belts that align with geomorphic structure, though some sharp local peaks are muted. The hybrid CNN-MLP reconciles these behaviors by preserving the CNN's spatial continuity while retaining sharper local maxima where tabular signals are informative, resulting in the most stable and interpretable map for planning and risk reduction.

All three models produced credible probability surfaces with distinct spatial character: the multilayer perceptron was fine-grained, the convolutional neural network formed smoother belts aligned with terrain, and the hybrid CNN-MLP combined both strengths. Performance ranked consistently hybrid highest, then CNN, then MLP showing a clear accuracy efficiency trade-off. In practice, MLP is fastest, CNN requires more compute, and CNN-MLP is slowest but delivers the most coherent and accurate maps when quality is the priority.

Permutation importance analysis was stable and consistent with geomorphic reasoning: elevation and slope were most influential, soil drainage and geology were secondary, aspect and forest cover had moderate effects, and curvature and stream power contributed modestly.

Overall, feature-level fusion of CNN and MLP offers a practical route to more accurate and spatially coherent landslide probability maps than single-branch baselines.

Although the results are promising, this study has several limitations. The landslide inventory is still relatively small, with only 163 documented events, which may limit the robustness and transferability of the models. Additionally, rainfall—one of the most important triggering factors—was not explicitly included in the current analysis. The modeling framework also focused solely on multilayer perceptron, convolutional neural network, and their combination, without testing more recent machine learning architectures. Future research should aim to expand the landslide database, incorporate rainfall characteristics, and compare a broader set of state-of-the-art models, including ensemble and advanced deep learning approaches, to further improve landslide spatial probability assessment.

Acknowledgement

This research is funded by Vietnam National University Ho Chi Minh City (VNU-HCM) under grant number DS2025-28-01.

Statements and Declarations

The authors declare that they have no known competing financial interests or personal relationships that could have appeared to influence the work reported in this paper.

References

[1] B.-Q.-V. Nguyen, L.-H.-P. Ho, Y.-T. Kim. (2024). An ensemble model of logistic regression, Naïve Bayes, and adaboost for assessing the landslide spatial probability-study case: Phuoc Son, Quang Nam, Vietnam and Umyeon, Seoul, Korea. *Civil Engineering and Architecture*, 12(3A), 2010–2028. DOI: 10.13189/cea.2024.121307

[2] B.-Q.-V. Nguyen, V.-L. Doan, Y.-T. Kim, C.-H. Song, J.-S. Lee. (2024). Considering antecedent rainfall to improve susceptibility assessment of rainfall-earthquake-triggered landslides on unsaturated slopes. *Environmental Earth Sciences*, 83, 142. https://doi.org/10.1007/s12665-024-11482-9

[3] B.-Q.-V. Nguyen, C.-H. Song, Y.-T. Kim. (2022). A Hybrid Physical and Machine Learning Model for Assessing Landslide Spatial Probability Caused by Raising of Ground Water Table and Earthquake in Atsuma, Japan—Case Study.

KSCE Journal of Civil Engineering, 26, 3416–3429. https://doi.org/10.1007/s12205-022-1656-2

[4] B.-Q.-V. Nguyen, Y.-T. Kim. (2021). Regional-scale landslide risk assessment on Mt. Umyeon using risk index estimation. *Landslides*, 18, 2547–2564. https://doi.org/10.1007/s10346-021-01622-8

[5] B.-Q.-V. Nguyen, Y.-T. Kim. (2021). Landslide spatial probability prediction: a comparative assessment of naive Bayes, ensemble learning, and deep learning approaches. *Bulletin of Engineering Geology and the Environment*, 80, 4291–4321. https://doi.org/10.1007/s10064-021-02194-6

[6] C.J. Van Westen. (2000). The modeling of landslide hazards using GIS. *Surveys in Geophysics,* 21, 241-255. https://doi.org/10.1023/A:1006794127521

[7] B.Y. Liao, S. Xie. (2022). Landslide Hazard Assessments of A Potential Earthquake-triggered in Central Taiwan Using Newmark's Model with the Stochastic Semi-Empirical Technique. *Civil Engineering and Architecture*, 10(7), 2877-2885. DOI: 10.13189/cea.2022.100708

[8] C.-H.-Q. Nguyen, T.-K. Nguyen, T.-H.-T. Vo, B.-Q.-V. Nguyen. (2023). Estimation of Shear Strength Parameters from Easily-Collected Soil Physical Properties Using Bagging Learning Technique. *International Journal of Membrane Science and Technology*, 10(1), 1105–1112. https://doi.org/10.15379/ijmst.v10i1.2751

[9] W. Chen et al. (2020). Evaluating the usage of tree-based ensemble methods in groundwater spring potential mapping. *Journal of Hydrology*, 583, 124602. https://doi.org/10.1016/j.jhydrol.2020.124602

[10] A. Merghadi et al. (2020). Machine learning methods for landslide susceptibility studies: A comparative overview of algorithm performance. *Earth-Science Reviews*, 207, 103225.https://doi.org/10.1016/j.earscirev.2020.103225

[11] B.T. Pham, B. Pradhan, D.T. Bui, I. Prakash, M.B. Dholakia. (2016). A comparative study of different machine learning methods for landslide susceptibility assessment: A case study of Uttarakhand area (India). *Environmental Modelling & Software*, 84, 240–250.https://doi.org/10.1016/j.envsoft.2016.07.005

[12] B.T. Pham, I. Prakash, D.T. Bui. (2018). Spatial prediction of landslides using a hybrid machine learning approach based on random subspace and classification and regression trees. *Geomorphology*, 303, 256–270. https://doi.org/10.1016/j.geomorph.2017.12.008

[13] H. Bilgilioğlu. (2023). A comparison of different machine learning models for landslide susceptibility mapping in Rize (Türkiye). *Baltica*, 36(2), 115-132. https://doi.org/10.5200/baltica.2023.2.3

[14] H.-Z. Cui, B. Tong, T. Wang, J. Dou, J. Ji. (2025). A hybrid data-driven approach for rainfall-induced landslide susceptibility mapping: Physically-based probabilistic model with convolutional neural network. *Journal of Rock Mechanics and Geotechnical Engineering,* 17(8), 4933-4951. https://doi.org/10.1016/j.jrmge.2024.08.005

[15] B.T. Pham, I. Prakash. (2019). A novel hybrid model of bagging-based naïve bayes trees for landslide susceptibility assessment. *Bulletin of Engineering Geology and the Environment*, 78, 1911–1925. https://doi.org/10.1007/s10064-017-1202-5

[16] A.M.S. Pradhan, Y.-T. Kim. (2017). Spatio-Temporal Landslide Hazard Mapping Using Coupled Hydrological Model in Mt Umyeon, Seoul. *Landscape Architecture and Regional Planning*, 2(3), 83-88. doi: 10.11648/j.larp.20170203.13

[17] A. Arabameri, S. Saha, J. Roy, W. Chen, T. Blaschke, D.T. Bui. (2020). Landslide susceptibility evaluation and management using different machine learning methods in the

Gallicash River Watershed, Iran. *Remote Sensing*, 12(3), 475. https://doi.org/10.3390/rs12030475

[18] D.T. Bui, O. Lofman, I. Revhaug, O. Dick. (2011). Landslide susceptibility analysis in the Hoa Binh province of Vietnam using statistical index and logistic regression. *Natural Hazards*, 59, 1413-1444. https://doi.org/10.1007/s11069-011-9844-2

[19] S. Haykin. (2009). Neural networks and learning machines. Prentice Hall.

[20] C.M. Bishop, N.M. Nasrabadi. (2006). Pattern recognition and machine learning. Vol. 4, No. 4. Springer.

[21] D.R. Roberts et al. (2017). Cross-validation strategies for data with temporal, spatial, hierarchical, or phylogenetic structure. *Ecography*, 40(8), 913–929. https://doi.org/10.1111/ecog.02881

[22] K. He, X. Zhang, S. Ren, J. Sun. (2015). Delving deep into rectifiers: Surpassing human-level performance on imagenet classification. *Proceedings of the IEEE International Conference on Computer Vision*, pp. 1026–1034.

[23] D.P. Kingma, J. Ba. (2014). Adam: A method for stochastic optimization. *arXiv*. https://doi.org/10.48550/arXiv.1412.6980

[24] Y. LeCun, Y. Bengio, G. Hinton. (2015). Deep learning. *Nature*, 521, 436-444. https://doi.org/10.1038/nature14539

[25] R. Girshick. (2015). Fast R-CNN. *Proceedings of the 2015 IEEE International Conference on Computer Vision (ICCV)*, pp. 1440–1448. doi: 10.1109/ICCV.2015.169

[26] H.-C. Shin et al. (2016). Deep convolutional neural networks for computer-aided detection: CNN architectures, dataset characteristics and transfer learning. *IEEE Transactions on Medical Imaging*, 35(5), 1285–1298. doi: 10.1109/TMI.2016.2528162

[27] X. Zhao, W. Chen. (2020). Optimization of computational intelligence models for landslide susceptibility evaluation. *Remote Sensing*, 12(14), 2180. https://doi.org/10.3390/rs12142180

[28] S. Jeong, Y. Kim, J.K. Lee, J. Kim. (2015). The 27 July 2011 debris flows at Umyeonsan, Seoul, Korea. *Landslides*, 12, 799–813. doi: 10.1007/s10346-015-0595-0

[29] M. Ercanoglu, C. Gokceoglu, T.W.J. Van Asch. (2004). Landslide susceptibility zoning north of Yenice (NW Turkey) by multivariate statistical techniques. *Natural Hazards*, 32, 1–23.https://doi.org/10.1023/B:NHAZ.0000026786.85589.4a

[30] L. Breiman. (2001). Random forests. *Machine Learning*, 45, 5–32. https://doi.org/10.1023/A:1010933404324

[31] A. Fisher, C. Rudin, F. Dominici. (2019). All models are wrong, but many are useful: Learning a variable's importance by studying an entire class of prediction models simultaneously. *Journal of machine learning research*, 20, 1–81.

[32] P. Reichenbach, M. Rossi, B.D. Malamud, M. Mihir, F. Guzzetti. (2018). A review of statistically-based landslide susceptibility models. *Earth-Science Reviews*, 180, 60–91. https://doi.org/10.1016/j.earscirev.2018.03.001

[33] C.J. van Westen, E. Castellanos, S.L. Kuriakose. (2008). Spatial data for landslide susceptibility, hazard, and vulnerability assessment: An overview. *Engineering Geology*, 102(3–4), 112–131. https://doi.org/10.1016/j.enggeo.2008.03.010

[34] D.R. Montgomery, W.E. Dietrich. (1994). A physically based model for the topographic control on shallow landsliding. *Water Resources Research*, 30(4), 1153–1171. https://doi.org/10.1029/93WR02979

[35] M. Iverson. (2000). Landslide triggering by rain infiltration. *Water Resources Research*, 36(7), 1897–1910,

[36] R. Sidle, H. Ochiai. (2006). Landslides: Processes, prediction, and land use. Water Resources Monograph Series. American Geophysical Union.

[37] L. Ma, Y. Liu, X. Zhang, Y. Ye, G. Yin, B.A. Johnson. (2019). Deep learning in remote sensing applications: A meta-analysis and review. *ISPRS Journal of Photogrammetry and Remote Sensing*, 152, 166–177. https://doi.org/10.1016/j.isprsjprs.2019.04.015

[38] X.X. Zhu et al. (2017). Deep learning in remote sensing: A comprehensive review and list of resources. IEEE Geoscience and Remote Sensing Magazine, 5(4), 8–36. doi: 10.1109/MGRS.2017.2762307

[39] I. Goodfellow, Y. Bengio, A. Courville. (2016). Deep learning. The MIT Press.